

Fraction of clogging configurations sampled by granular hopper flow

C. C. Thomas and D. J. Durian

Department of Physics and Astronomy, University of Pennsylvania, Philadelphia, PA 19104-6396, USA

(Dated: December 7, 2024)

We measure the fraction F of grain configurations that cause granular hopper flow to clog, based on the average mass discharged between clogging events for apertures of various sizes, shapes, and orientations. By tilting the hopper, we demonstrate that F is a function of the hole area projected in the direction of the exiting grain velocity. By varying the length of slits, we demonstrate that grains clog in the same manner as if they were flowing out of a set of smaller independent circular openings. Finally, we find that the fraction of stable microstates of individual grains in the clogging region is a constant for large opening sizes. This is consistent with a model in which F decays exponentially in hole width raised to the power of the system dimensionality. As such, there is no sharp clogging transition, and all hoppers have a nonzero probability to clog.

PACS numbers: 45.70.Ht, 45.70.Mg

Granular flow through a small hole or bottleneck is susceptible to clogging, where a stable arch forms over the hole and arrests the flow [1–3]. Clogging is a highly useful phenomenon to test the extreme limits of granular flow. In clogging, the bulk continuum-like behavior of an arbitrarily large system is governed by the discrete rearrangements of a small quantity of particles at the exit. Furthermore, clogging demonstrates the behavior of a system that evolves spontaneously from a freely-flowing state to a jammed state with no change in the external forcing. Similar phenomena are important for understanding the flow of emulsions [4] or granular suspensions [5, 6] through constrictions, the flow of vortices through an array of pinning sites in type II superconductors [7, 8], automotive traffic jams [9] and pedestrian traffic [10]. In spite of many simulations [11–14] and experiments in both two- [1, 15–19] and three-dimensional hoppers [2, 3, 12, 20–23] in recent years, very little is understood about how to predict or control clogging.

A valuable measure commonly used to quantify clogging is the average mass $\langle m \rangle$ discharged before a clog occurs. Fig. 1 displays data from Ref. [23], showing how $\langle m \rangle$ grows extremely rapidly with hopper hole diameter D for several different tilt angles θ . Various forms for $\langle m \rangle$ versus D have been proposed. Refs. [3, 17, 23] fit the data to a critical power law (long dashed curves on Fig. 1), diverging at finite $D = D_c$. However, there is no model for the value of D_c or the exponents, which are in the range of 2 – 12. Furthermore, other data show that $\langle m \rangle$ grows in proportion to $\exp(CD^2)$ in two-dimensional systems [16, 17] or $\exp(CD^3)$ in a three-dimensional system (solid curves on Fig. 1) [23]. The exponential form is somewhat better in describing the Ref. [23] data, since the ratio of χ^2 for the diverging form to its value for the exponential form falls mainly in the range 0.7 – 1.9. The conflict between these different forms is significant. If $\langle m \rangle$ diverges at finite D , then there exists a sharp clogging transition marking a regime where the flow will *never* clog.

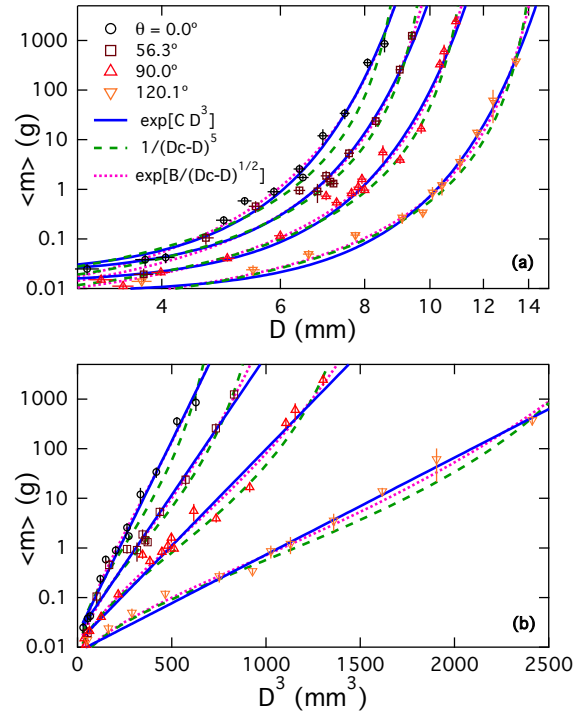


FIG. 1: (Color online) Average mass $\langle m \rangle$ discharged before a clog forms, illustrated as a function of (a) hole diameter D and (b) D^3 for $d = 2$ mm glass beads in hoppers with different tilt angles as labeled. These data are from Ref. [23], and are well fit by different functional forms, as labeled.

To clarify the nature of clogging, we propose a more fundamental quantity: the fraction F of grain configurations near the exit that will clog the flow. We argue how F may be deduced from $\langle m \rangle$ and test our approach by varying the geometry, first by tilting the hopper and also by varying the length L of a slit. We make no assumptions about the distance that grains move between rearrangements, but find that it is approximately one grain diameter. We find that F for spherical grains of

TABLE I: The mean grain diameter d , the bulk density ρ , and the draining angle of repose θ_r for the grains tested. Errors for d indicate the standard deviations of the distributions. For the other material properties, error bars indicate the standard error in the measurements.

Material	d (mm)	ρ (g/cm ³)	θ_r
Glass Spheres	2.02 ± 0.04	1.62 ± 0.01	$23.5 \pm 0.5^\circ$
Glass Spheres	0.96 ± 0.05	1.56 ± 0.02	$20.0 \pm 0.4^\circ$
Dry Tapioca	3.50 ± 0.14	0.69 ± 0.01	$32.3 \pm 0.5^\circ$

cross-sectional area A_g is a single function of an effective normalized aperture area A_{eff}/A_g .

We conduct our experiments with three different spherical grains and three different hopper shapes. The material properties of the grains, including the grain diameter d , bulk density ρ , and draining angle of repose θ_r , are listed in Table I. To explore the clogging of grains at a circular hole, we use an aluminum hopper with smooth sidewalls and floor and inner cross-section of dimensions 9.5×9.5 cm². The hole is a camera iris with continuously adjustable diameter D . We also change the propensity to clog by tilting this hopper, varying the angle θ that the hole makes with gravity. When $\theta > 60^\circ$, the iris is mounted on the sidewall of the hopper rather than its floor; however, this does not affect the behavior of the flow or clogging. We use the 2 mm glass spheres when investigating clogging in this hopper. The data presented for clogging in this hopper were previously published in Ref. [23].

To explore the effect of the aperture shape, we investigate clogging from a rectangular slit of long dimension L and short dimension D . As with the circular hole, we use a hopper with smooth floor and sidewalls. The inner cross-section of this hopper is 28×20 cm². To vary D , we use a custom-made aluminum slit that allows for fine control over the width while maintaining a constant length. Data collected for the 1 mm glass spheres for this slit with $L = 149$ mm were previously reported in Ref. [23]. However, we now also change the slit length by masking the sides of the slit. We investigate the effect of changing L and D using both the 1 mm and 2 mm glass spheres.

Finally, we report on clogging for a somewhat different slit geometry and material. This third hopper has a slit of constant length $L = 3.8$ cm and adjustable width D . However, the inner dimensions of the hopper are 3.8×56 cm² and thus two of the inner walls coincide with the ends of the slit. Furthermore, we inhibit the sliding of grains along the bottom of the hopper by placing two grain-size dowels at the lips of the slit. For this hopper we use 3.5 mm diameter dry tapioca pearls.

To determine the fraction F of configurations that may clog a hole, we begin by noting that the distribution of flow durations τ , and also therefore of discharge masses

m , is exponential: $P(\tau) = \exp(-\tau/\langle\tau\rangle)$, where $\langle\tau\rangle$ is the average duration of flow events [2, 3, 15–19, 23]. Thus clogging is a Poisson process, and the probability to remain unclogged across a time increment is $1 - dt/\langle\tau\rangle$. The average mass discharged is $\langle m \rangle = \rho A v \langle \tau \rangle$, where ρ is the bulk mass density of the medium, v is the average flow speed of the exiting grains, and A is the aperture area. The shortest relevant time increment is the sampling time τ_0 needed for grain configurations to change. Then $F = \tau_0/\langle\tau\rangle$ is the fraction of configurations that form a stable arch over the aperture. The grains near the hole move down a distance $\ell = v\tau_0$ between successive configuration changes. Altogether, this gives the fraction F of stable configurations as

$$F = \rho A \ell / \langle m \rangle, \quad (1)$$

which may be deduced by measuring the quantities on the right-hand side.

In order to determine the sampling length ℓ , we assume F approaches one as the aperture area A is reduced to the size of one grain. We plot $\rho A d / \langle m \rangle$ versus $A - A_g$ in Fig. 2a, where A_g is the cross-sectional area of a single grain. We do this for the 2 mm glass spheres clogging at a circular hole. We also include data for tilted hoppers, where A is replaced by an effective area defined by the projection of the hole $A\hat{n}$ in the average flow direction \hat{v} :

$$A_{\text{eff}} \equiv (A\hat{n}) \cdot \hat{v} = A \begin{cases} \cos \theta & \theta \leq \theta_r \\ \cos[(\theta + \theta_r)/2] & \theta \geq \theta_r \end{cases} \quad \begin{matrix} (2a) \\ (2b) \end{matrix}$$

where θ_r is the draining angle of repose (see Table I) and θ is the angle between the hole normal \hat{n} and vertical [23]. Fig. 2a demonstrates that $Fd/\ell = \rho A_{\text{eff}}d/\langle m \rangle$ is linear in $A_{\text{eff}} - A_g$ for various tilt angles θ . For each θ independently, we fit the data to a linear form (not shown). The y -intercepts for these fits are then the values of d/ℓ for each θ . The values of ℓ/d determined in this manner are independent of θ , as shown on Fig. 2b. Averaging over θ gives an estimate of the sampling length that is slightly less than one grain diameter, as expected: $\ell = (0.70 \pm 0.04)d$. The simultaneous linear fit for all θ using this value of ℓ/d is shown as the solid line on Fig. 2a, with the grey band indicating the fitting confidence interval.

We now find F for the 2 mm glass spheres in the tilted hopper. To do so, we use the above value of ℓ/d with the measured average discharged mass $\langle m \rangle$ for circular holes of different diameters D and tilt angles θ . Fig. 3a shows F as a function of the effective hole area A_{eff}/A_g . The data points in this plot are shaded by $\hat{v} \cdot \hat{n}$. These values of F for circular holes fall off rapidly by many orders of magnitude with increasing A_{eff}/A_g . Furthermore, there is apparently no dependence of F on θ , such that F is a single function of A_{eff}/A_g .

Next we consider rectangular slits of long dimension L and short dimension D , at $\theta = 0$. We hypothesize that

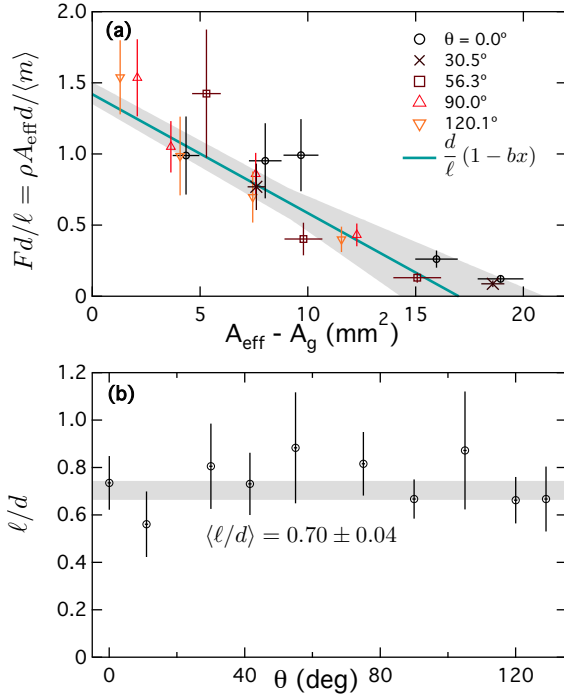


FIG. 2: (Color online) (a) $\rho A_{\text{eff}} d / \langle m \rangle$ versus $A_{\text{eff}} - A_g$ for tilted hoppers, where ρ is the bulk density of the grains, d is the grain diameter, $\langle m \rangle$ is the average mass discharged before clogging, A_{eff} is the effective hole area for a tilted hopper, and A_g is the cross-sectional grain area. According to Eq. (1), the quantity plotted is equal to Fd/ℓ , where ℓ is the sampling length. (b) Sampling length ℓ/d versus tilt angle θ , as found from linear fits to data as displayed in part (a). The average value $\langle \ell \rangle = (0.70 \pm 0.04)d$ is indicated. The simultaneous linear fit for all angles using this value of ℓ/d is overlaid on (a), with the confidence bands indicated by the grey swath.

slits behave as a collection of $(4/\pi)L/D$ independently clogging circular holes of diameter D . If this is so, then

$$F_{\text{slit}}(D, L) = [F_{\text{circle}}(D)]^{(4/\pi)L/D}. \quad (3)$$

We therefore determine the value of F for circular holes of diameter D based on the measured values of $\langle m \rangle$ for rectangular slits of width D . These data are displayed on Fig. 3b versus $A = \pi D^2/4$, where D is the slit width and the aspect ratio L/D is indicated by shading. This analysis causes the data in Fig. 3b, for the different grain types and a wide range of slit widths and aspect ratios, to all fall onto a single curve.

Finally, we compare F for circular holes (Fig. 3a) with the circular components which constitute the rectangular slits (Fig. 3b) by simultaneously fitting both data sets to two empirical forms:

$$F(x) = \begin{cases} \left(\frac{x_c^\gamma - x^\gamma}{x_c^\gamma - 1} \right)^\beta \\ \exp \left[-C \left(x^{\alpha/2} - 1 \right) \right], \end{cases} \quad (4)$$

$$(5)$$

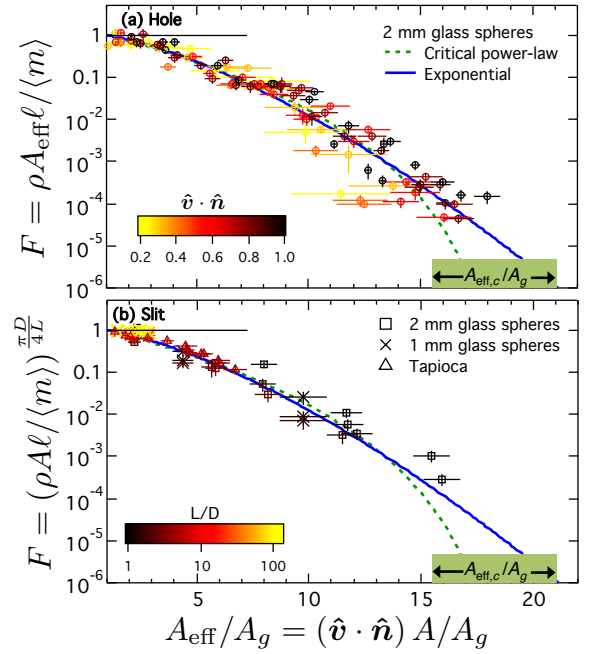


FIG. 3: (Color online) Fraction of clogged configurations, deduced from measurements of $\langle m \rangle$, versus normalized effective hole area. Data for circular holes (a) are shaded by $\hat{v} \cdot \hat{n}$. Data for the circular subsections of rectangular slits (b) are shaded by slit aspect ratio L/D . The clogging transition locations found from critical power law fits in Ref. [23] for the 2 mm glass spheres are indicated by $A_{\text{eff},c}/A_g$ at bottom right. The best fits to Eq. (4) and Eq. (5) are overlaid as dashed and solid curves, respectively.

where $x \equiv A_{\text{eff}}/A_g$. For the best critical power-law fit to both hole and slit data, we find $\gamma = 1.0 \pm 0.2$, $\beta = 6.0 \pm 0.3$, and $x_c = 19.1 \pm 0.3$. This fit is shown by the dashed curve in Fig. 3a and 3b. Note that the critical aperture size x_c is within the range of the observed values for the clogging transition reported in Ref. [23], indicated on the lower right of Fig. 3. For the best simultaneous exponential fit to both hole and slit data, we find $\alpha = 3.0 \pm 0.2$ and $C = 0.14 \pm 0.03$. This result is shown by the solid curve in Fig. 3a and 3b. Note that the two fitting forms describe both data sets equally well, as the ratio of χ^2 for the fit to Eq. (4) to its value for the fit to Eq. (5) is 1.06. Thus, the data collapse onto a single function of A_{eff}/A_g . However, as in Fig. 1, the multitude of good empirical fitting forms makes it unclear whether or not there is a sharp clogging transition where $F(x)$ vanishes at finite x_c .

While there is no theory for Eq. (4), we can predict Eq. (5) from a simple model based on the possible microstates of individual grains near the aperture. To begin we suppose that the number of grains in the clogging region above the hole must scale as $N = (D/d)^\alpha$, where α could depend on dimensionality. If each of these N grains could be in V_1 single-grain position and momen-

tum microstates, then the total number of allowed configurations is $\Omega \propto V_1^N$. And if only a certain number V_s of the microstates are stable, or precede a clog, then the total number of stable configurations is $\Omega_s \propto V_s^N$. Then, from $F \equiv \Omega_s/\Omega$, we find:

$$F = \left(\frac{V_s}{V_1}\right)^N = \exp \left[- \left(\ln \frac{V_1}{V_s} \right) \left(\frac{D}{d} \right)^\alpha \right]. \quad (6)$$

This is precisely Eq. (5) for large A_{eff}/A_g and $\alpha = 3.0 \pm 0.2$. For our data in three dimensions, and also for the $\langle m \rangle \propto \exp(CD^2)$ data in two dimensions [16, 17], we thus have a consistent picture in which the fraction of clogged configurations dies exponentially with hole width raised to the power α equal dimensionality. The value of α implies that more grains are involved in arch formation and stability than just those exposed underneath. This is consistent with observations that an obstacle placed over the aperture has no influence on clogging or discharge if it is higher than about two hole widths [19].

The above model for F is highly simplified, but can be used to estimate the ratio V_s/V_1 of single-grain microstates within the clogging region that are stable, or precede a clog. First, for large A_{eff}/A_g , comparison of Eq. (6) and the fit to Eq. (5) gives $V_s/V_1 = \exp(-C) = 0.87 \pm 0.03$. More generally, we can deduce the ratio from $V_s/V_1 = F^{1/N}$ using $N = (\hat{\mathbf{v}} \cdot \hat{\mathbf{n}})(D/d)^3$. The results from all hole and slit data are plotted in Fig. 4. For small hole sizes, all microstates are stable and V_s/V_1 approaches 1. With increasing hole size, V_s/V_1 does not vanish but instead quickly approaches a nonzero constant 0.87 ± 0.03 . This value is perhaps surprisingly close to one. It means that each grain near the exit is almost always in a position to participate in a clog, which is consistent with the flows being very dense and not far dilated from random-close packing. For large enough hole sizes, actual clog formation is rare because *all* the grains in the region must be suitably positioned. Perhaps V_s/V_1 represents the ratio of stable- to free- volume, or perhaps momentum states are important too. The detailed nature of single-grain microstates, the importance of collective effects, the size of the clogging region, and more, could be studied by simulation.

To conclude, prior fits to critical power laws [3, 17, 23] and the seeming universality of the clogging phase diagram [23] were strong arguments for the existence of a sharp clogging transition at a finite hole size D_c . However, lack of theory for exponents and maximum hole size, and the absence of diverging quantities on approach to D_c from above, were all causes for concern. Here, based on a probabilistic analysis and modeling of new and old data, we find compelling reasons to view clogging as always possible. The act of flow causes a random sampling of configurations for grains above the hole in a region of size given by hole width raised to the power of dimensionality. Flow proceeds until a configuration arises in

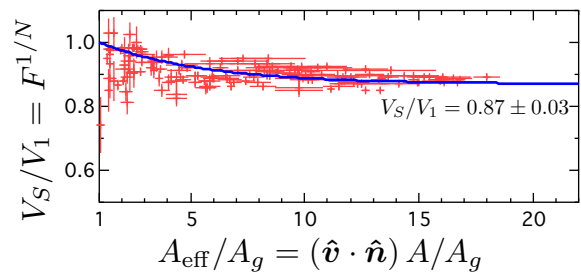


FIG. 4: (Color online) Ratio of the stable to total single-grain microstates versus normalized effective hole area, obtained for *all* the data shown in Fig. 3 by computing $F^{1/N}$ where $N = (\hat{\mathbf{v}} \cdot \hat{\mathbf{n}})(D/d)^3$. For moderately large holes, V_s/V_1 falls to a constant value 0.87 ± 0.03 , as illustrated by the exponential fit shown in blue.

which *all* these grains are able to participate in forming a stable arch, or dome. This naturally gives an exponential distribution of discharge event sizes. And since the probability for a given grain to be able to participate in a clog is constant, independent of hole size, there is no critical hole size beyond which the system is no longer susceptible to clogging. Instead, the average flow duration increases dramatically, exponentially, due to the increasingly large number of grains that are required to occupy stable microstates. Clogging is thus similar to the glass and jamming transitions, which are defined by an observation threshold. There, relaxation times increase dramatically and can be fit to a variety of forms, some of which diverge and some of which do not. The same can be said for clogging. There is no critical point, but as a practical matter a clogging transition may still be defined at the hole size beyond which clogging becomes so vastly improbable as to be unobservable.

This work was supported by the NSF through Grant No. DMR-1305199. We thank R. P. Behringer and E. Clément for helpful discussions and impressing on us the possibility that $\langle m \rangle$ does not diverge at finite hole size.

-
- [1] K. To, P.-Y. Lai, and H. K. Pak, Phys. Rev. Lett. **86**, 71 (2001).
 - [2] I. Zuriguel, L. A. Pugnaloni, A. Garcimartín, and D. Maza, Phys. Rev. E **68**, 030301 (2003).
 - [3] I. Zuriguel, A. Garcimartín, D. Maza, L. A. Pugnaloni, and J. M. Pastor, Phys. Rev. E **71**, 051303 (2005).
 - [4] D. Chen, K. W. Desmond, and E. R. Weeks, Soft Matter **8**, 10486 (2012).
 - [5] J. R. Valdes and J. C. Santamarina, SPE Journal **11**, 193 (2006).
 - [6] N. Roussel, T. L. H. Nguyen, and P. Coussot, Phys. Rev. Lett. **98**, 114502 (2007).
 - [7] C. J. Olson Reichhardt and C. Reichhardt, Phys. Rev. B **81**, 224516 (2010).
 - [8] C. J. Olson Reichhardt, E. Groopman, Z. Nussinov, and C. Reichhardt, Phys. Rev. E **86**, 061301 (2012).

- [9] B. S. Kerner and H. Rehborn, Phys. Rev. E **53**, R4275 (1996).
- [10] D. Helbing, I. Farkas, and T. Vicsek, Nature **407**, 487 (2000).
- [11] S. S. Manna and H. J. Herrmann, Eur. Phys. J. E **1**, 341 (2000).
- [12] L. Pournin, M. Ramaioli, P. Folly, and T. M. Liebling, Eur. Phys. J. E **23**, 229 (2007).
- [13] S. Tewari, M. Dichter, and B. Chakraborty, Soft Matter **9**, 5016 (2013).
- [14] L. Kondic, Granular Matter **16**, 235 (2014).
- [15] E. Clément, G. Reydellet, F. Rioual, B. Parise, V. Fanguet, J. Lanuza, and E. Kolb, in *Traffic and Granular Flow '99*, edited by D. Helbing, H. Herrmann, M. Schreckenberg, and D. Wolf (Springer, Berlin, 2000), pp. 457–468.
- [16] K. To, Phys. Rev. E **71**, 060301 (2005).
- [17] A. Janda, I. Zuriguel, A. Garcimartín, L. A. Pugnaloni, and D. Maza, Europhys. Lett. **84**, 44002 (2008).
- [18] J. Tang, S. Sagdiphour, and R. P. Behringer, AIP Conf. Proc. **1145**, 515 (2009).
- [19] I. Zuriguel, A. Janda, A. Garcimartín, C. Lozano, R. Arévalo, and D. Maza, Phys. Rev. Lett. **107**, 278001 (2011).
- [20] A. Drescher, A. J. Waters, and C. A. Rhoades, Powder Technol. **84**, 177 (1995).
- [21] H. G. Sheldon and D. J. Durian, Granular Matter **12**, 579 (2010).
- [22] S. Saraf and S. V. Franklin, Phys. Rev. E **83**, 030301 (2011).
- [23] C. C. Thomas and D. J. Durian, Phys. Rev. E **87**, 052201 (2013).